Detection of Cysteine with Glutathione-capped Silver Nanoparticles in the Presence of Ni^{2+} Ions

CAN SERKAN KESKIN[1], SEMRA YILMAZER KESKIN[1], ABDIL ÖZDEMIR[1]*
Department of Chemistry, Faculty of Arts & Science, Sakarya University, 54100 Sakarya, Turkey

Glutathione-capped silver nanoparticles (AgGSH) were prepared by the reduction of silver nitrate using $NaBH_4$, and then were used for the detection of cysteine (Cys) in aqueous solution in the presence of Ni^{2+} ions via absorption properties of the resulting structures. The synthesized and modified nanoparticles were characterized by IR spectroscopy, ultraviolet-visible (UV-Vis) spectroscopy, and atomic force microscopy. UV-Vis spectroscopy is an effective characterization method because the AgGSH-Ni nanoparticles show intense surface plasmon resonance bands in the presence of Cys. The sensitivity of AgGSH-Ni nanoparticles toward other amino acids is negligible. Therefore, it is highly selective for detecting Cys in aqueous solutions. The AgGSH-Ni surface plasmon absorption linearly increases with the Cys concentrations in the range from 1×10^{-4} to 1×10^{-3} M. Furthermore, the detection limit of Cys is 1×10^{-5} M.

Keywords: Silver nanoparticles; glutathione; cysteine, amino acids; nanoparticles; AFM.

Modified nanoparticles attract considerable interest due to their applications in a wide variety of fields such as glucose detection with 3-(aminopropyl) triethoxysilane and glucose oxidase modified magnetic nanoparticles [1], bovine serum albumin detection with N-methyl-D-glucamine-modified silica nanoparticles [2], and the destruction of chlorinated solvents with carboxymethyl-cellulose-modified iron nanoparticles [3]. Thiol groups have been utilized for the surface modification of nanoparticles [4–6], especially silver nanoparticles, due to the high affinity of -SH groups toward silver atoms [7, 8]. Glutathione (GSH) is an intercellular tripeptide consisting of γ-glutamic acid-cysteine-glysine amino acids and a thiol group [9]. GSH-modified nanoparticles have been used in many studies such as the synthesis of CdS nanocrystals [10], cell-imaging applications of CdTe quantum dots [11], and colorimetric detection of Ni^{2+} [12].

L-cysteine (Cys) is an amino acid widely used in the food and pharmaceutical industries. Abnormally high levels of Cys in blood can cause hyperhomocysteinemia and diseases such as Alzheimer's and Parkinson's [13, 14]. Several Cys detection methods such as flow injection analysis [15], high-performance liquid chromatography [16], gas chromatography and mass spectrometry [17], ion-exchange chromatography [18], spectrophotometry based on ninhydrin [19], 2-vinylquinoline [20] and fluoropyruvic acid reactions [21], extraction with butyl alcohol [22], chemiluminescence [23], potentiometry with silver-mercury electrodes [24], voltammetry with diamond electrodes [25], and capillary electrophoresis [26] have been reported. Nanoparticles can also be used for detecting Cys. It was reported the detection of Cys by a resonance light scattering technique that is based on the interactions between the NH_3^+ group on Cys and the -SH groups on the gold nanoparticles via covalent combination with –SH group and electrostatic binding with the $–NH_3^+$ group of Cys [27]. Near-infrared fluorescence detection of Cys using gold nanoparticles, which is based on the strong affinity of thiols toward gold was reported [28]. Sudeep et al. have reported Cys and GSH detection using gold nanorods based on the interaction between the -SH groups of GSH and the gold nanorods [29].

In this paper, we present a new methodology for the detection of Cys in aqueous solutions by using GSH-modified silver nanoparticles (AgGSH). For the detection of other amino acids, similar methods have been reported in the literature [30]. In the proposed method, the interaction of AgGSH nanoparticles with amino acids is relatively weak; however, the nanoparticles can bind to metal ions (e.g., Ni^{2+}), which can interact with the amino acid ligand. Therefore, the metal ions bind both the AgGSH nanoparticles and the amino acid molecules through cooperative metal–ligand interactions. In this complex, the three components exist together and the selectivity of the method is determined by the binding affinity between the metal center and the amino acid. In this study, we show that the interaction of the AgGSH nanoparticles with Cys is very selective and sensitive in the presence of Ni^{2+} ions.

Experimental part

Materials

All chemicals used were of analytical grade or of the highest purity available. Silver nitrate ($AgNO_3$), sodium borohydride ($NaBH_4$), and $Ni(NO_3).6H_2O$ were purchased from Merck Chemicals, and GSH was purchased from Fluka. Twenty amino acids were used. L-alanine was purchased from Fluka; L - arginine, L-aspartic acid, L- glutamine, glycine (Gly), L-histidine, L - isoleucine, L-leucine, L - methionine, L - phenylalanine, L - proline, L-serine, L-tyrosine, and L-valine were purchased from Merck; L-asparagine, L-cysteine (Cys), L -glutamic acid, L-lysine, L-threonine, and L-tryptophan were purchased from Sigma. All solutions were prepared with double distilled deionized water (Millipore 18 M cm^{-1} resistance) and were stored at room temperature. The concentration of nickel ions is 1×10^{-3} M. All glassware were cleaned with a diluted HNO_3 solution and rinsed with Mill-Q water prior to use.

Synthesis of AgGSH nanoparticles

GSH-capped silver nanoparticles were synthesized according to the published methods [12, 30, 31]. $NaBH_4$ (0.01 g) was added to a concentrated aqueous solution of $AgNO_3$ (100 mL, 1×10^{-4} M) at room temperature in order

* email: abdilo@sakarya.edu.tr; Tel.: +902642956046

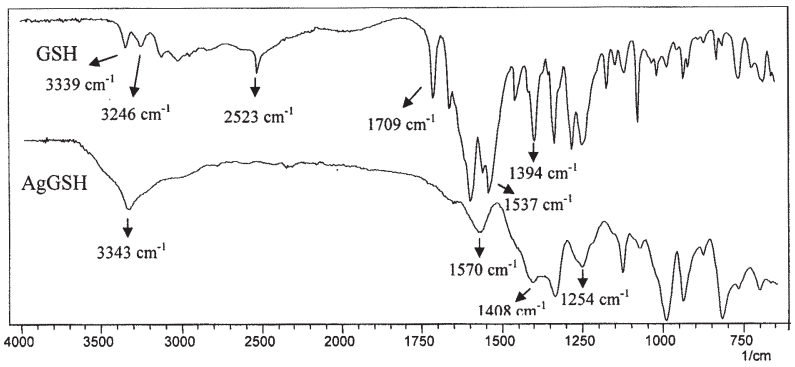

Fig. 1. FTIR spectra of GSH and AgGSH nanoparticles

to reduce silver ions. After stirring for 5 min to provide a homogeneous nucleation, an a queous solution of GSH (2 mL, 1 × 10^{-3} M) was added to stabilize the silver nanoparticles. After aging the silver colloidal solution for 2 h, AgGSH nanoparticles were obtained and stored in the dark.

Characterization

UV-Vis absorption spectra were obtained by UV-Vis spectrophotometry (Shimadzu UV-Vis 160A) by measuring the full absorption spectrum of mixtures in the range of 200–800 nm. FTIR spectra were measured with a Schimadzu IR Prestige-21 spectrometer. The morphology of the synthesized and modified nanoparticles were characterized by atomic force microscopy (AFM) using a NTMDT Integra instrument. Nanoparticles were dispersed in a suitable amount of methanol and vortexed for 15 min to prepare a homogeneous dispersion. Then, a drop of the sample was spread on a glass surface and left to dry before performing the AFM measurement.

Results and discussions

GSH-capped silver nanoparticles have a significant role in Cys sensor fabrication. It has three different ionic forms, namely, zwitterionic, cationic (-NH_3^+) via protonation, and anionic (-COO^-, -S^-, -COO^-) via deprotonation. Chemisorption of GSH on gold nanoparticles was previously investigated [32]. The researchers showed that the zwitterionic form binds to the nanoparticle via the -SH and -COO^- groups. Upon the addition of acid, the carboxylic acid groups are protonated. This means that in the gly part of GSH, the interaction between the carboxylate and the gold surface is lost upon protonation and only the -SH interaction remains. Basu et al. [33] and Lim et al. [34] supported the formation of this proposed structure and the same bond interactions are valid for silver nanoparticles and GSH molecules.

Characterization of AgGSH nanoparticles

The interaction between GSH and nanoparticles was studied by FTIR spectroscopy. The IR spectra of GSH and AgGSH are presented in figure 1. The results indicate that GSH shows a strong band at 2523 cm^{-1} because of the -S-H stretching vibrations; this band is absent in the spectra of AgGSH, indicating deprotonation and coordination of the thiol group [35]. In GSH, the band at 1709 cm^{-1} is attributed to the -COOH group of the glycine residue, which is absent in AgGSH. This indicates interaction of -COOH with metal ions.

The key factor for this binding is the *p*H of the solution (8.45 for synthesized nanoparticles), which affects the protonation or deprotonation of the -COOH group. The deprotonated -COOH group binds to the nanoparticles. In the AgGSH complex, the doublet peaks of GSH for the symmetric stretching vibrations of the -NH_2 group observed at 3246 cm^{-1} and 3339 cm^{-1} merge into a single band around 3343 cm^{-1}. The -N-H stretching frequency in the 3125–2900 cm^{-1} region corresponding to the free ligand, which is hydrogen bonded to the zwitter ion -OOC-C-NH_3^+ of the amino acid [36], does not show any considerable shift in AgGSH; this indicates non-participation of the N-H group.

These free groups aggregate the AgGSH particles in the solution [37]. Figure 2 shows 2D-topographic AFM image of the assembly of aggregated silver nanoparticles, mediated by 0.001 M GSH, deposited on a glass after dispersing in methanol and scanner area is 100 μm^2. In GSH, the C=O and C-O stretching frequencies at 1537 cm^{-1} and 1394 cm^{-1} are attributed to the symmetric and asymmetric modes of the -COO- group, respectively. In AgGSH, these bands considerably shift to 1408 cm^{-1} and 1254 cm^{-1}, respectively, confirming that binding occurs.

The synthesized AgGSH nanoparticles were also analyzed using UV-Vis measurements. The freshly prepared AgGSH nanoparticles have an absorption peak at 395 nm (fig. 3). The absorption peak decreases in intensity and the plasmon band broadens with time because of particle aggregation.

This continued for 15 days, and then in the following 30 days, there was no obvious change in the absorption peak. The absorption spectra of the nanoparticles showed significant broadening after 60 days (fig. 3) due to the aggregation of the modified nanoparticles in the solution. Figure 6 shows the effect of changing *p*H on the stability of the AgGSH nanoparticles. Based on the experimental results (fig. 4), the freshly synthesized nanoparticles are highly stable at *p*H > 6. Under these pH conditions, GSH is in the anionic form owing to the deprotonation of the

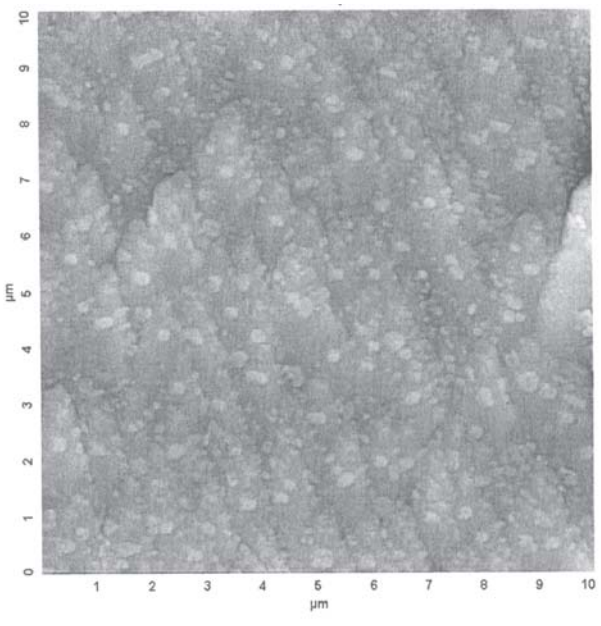

Fig. 2. AFM topographical image of AgGSH nanoparticles

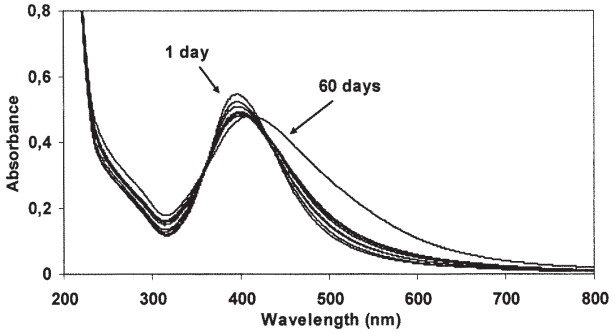

Fig.3. Changes in absorption of AgGSH nanoparticles with time

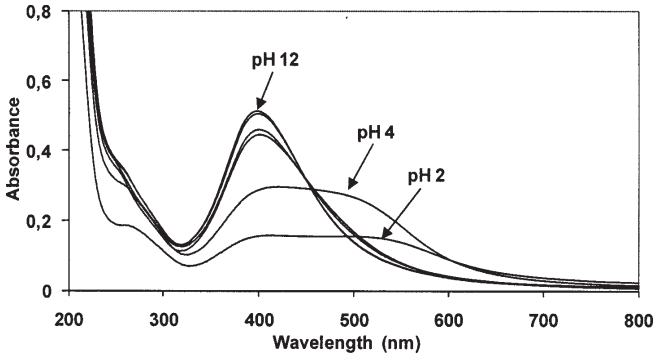

Fig. 4. Changes in the absorption of AgGSH nanoparticles with *p*H

-COOH group. Furthermore, the synthesized nanoparticles are quite stable probably because of the strong interparticle electrostatic repulsions between the carboxylate anions of the GSH-capped silver nanoparticles.

At lower *p*H values, GSH is in the cationic form because of the protonation of the $-COO^-$ and $-NH_2$ groups. Moreover, the AgGSH nanoparticle plasmon absorption band showed significant broadening on account of hydrogen bonding. At neutral *p*H values, GSH is in the zwitter ionic form due to the $-COO^-$ and $-NH_3^+$ groups [32].

Detection of Cys in the presence of Ni^{2+} by AgGSH particles

Figure 5 shows the absorption spectra of 20 amino acids in the presence of AgGSH nanoparticles and Ni^{2+} ions (1×10^{-3} M). For each measurement, 1 mL amino acid and 1 mL Ni^{2+} solutions were added to the AgGSH solution. None of the solutions showed obvious absorption changes, suggesting that among the amino acids only Cys interacts with the nanoparticles. When Cys is added to the solutions, two absorption peaks appeared; one at around 395 nm, and the other at 270.1 nm, suggesting interactions among the AgGSH nanoparticles, Ni^{2+} ion, and Cys. In figure 5, tryptophan and tyrosine show distinct absorption peaks at 278.5 nm and 274 nm, respectively, due to absorption of

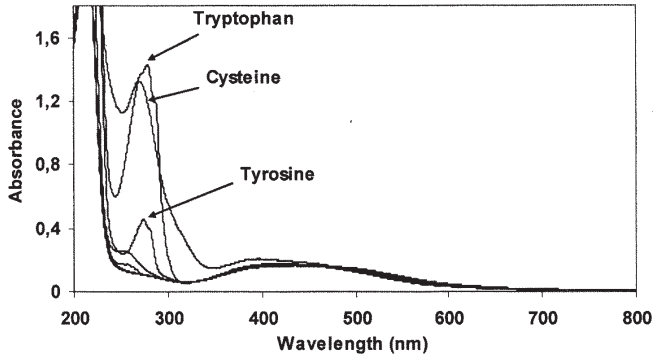

Fig. 5. Absorption spectra of 20 amino acids in the presence of Ni^{2+} and AgGSH nanoparticles

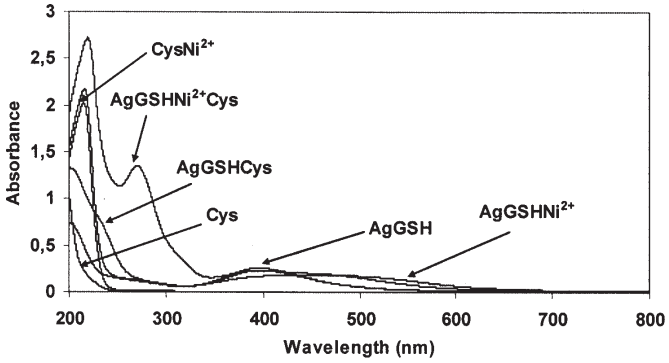

Fig. 6. Absorption spectra of Cys, AgGSH, AgGSHCys, $AgGSHNi^{2+}$, $CysNi^{2+}$, and $AgGSHNi^{2+}Cys$ solutions

benzene groups of amino acids. These peaks not as a result of interactions among the AgGSH nanoparticles, Ni^{2+} ion, and amino acids and they do not interfere with the quantitative studies of Cys.

The UV-Vis absorption spectra of Cys, AgGSH, AgGSH-Cys, AgGSH-Ni^{2+}, Cys-Ni^{2+}, and AgGSH-Ni^{2+}-Cys solutions verified the AgGSH-Ni^{2+}-Cys interactions. To further clarify the existence of interactions among AgGSH, Ni^{2+}, and Cys, the absorption spectra of different solutions were measured and are summarized in figure 6. Cys (1×10^{-3} M) does not show significant absorption peaks. The AgGSH absorption spectrum has a peak at around 395 nm which decreases with the addition of Cys to the solution this is because of the binding of Cys to the silver nanoparticles via the thiol group.

In the presence of Ni^{+2} ions, a broad peak was observed from 393 to 503 nm because of the AgGSH-Ni^{2+} interactions which indicates the aggregation of AgGSH nanoparticles. As expected, Cys forms a complex with Ni^{+2} ions in the solution with absorption peak at around 214 nm. In the case of the AgGSH-Ni^{2+}-Cys complex, a distinct absorption peak was observed at 270 nm. For the other combinations no significant interference absorption peaks were observed. These findings support the development of a new detection method for Cys in solutions in the presence of other amino acids.

The AgGSH nanoparticles selectively bind to Cys in the presence of Ni^{+2}. The absorption spectra of the AgGSH-Ni^{2+}-Cys complex show a linear dependence on Cys concentrations. Using this linear relationship, we developed a method to quantitatively determine the concentration of Cys. Figure 7 shows the typical absorption spectra of aqueous solutions containing Ag-GSH nanoparticles, Ni^{2+} ions, and different concentrations of Cys.

The UV-Vis spectra indicate the change in the absorption spectra of solutions with increasing concentrations of Cys. To develop a new detection method and to investigate the

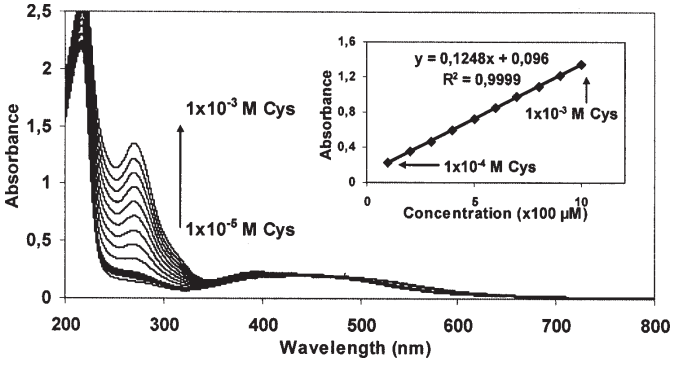

Fig. 7. Changes in absorption in the Ni^{2+} and AgGSH nanoparticle solution with different concentrations of Cys.

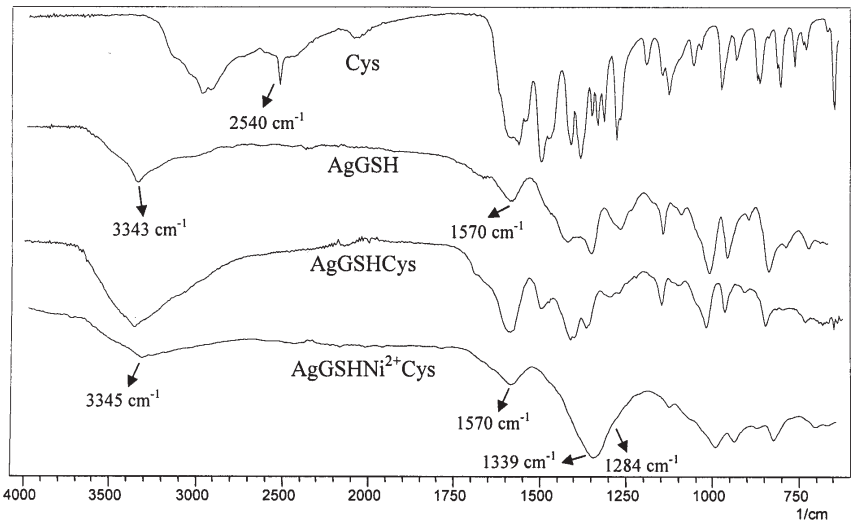

Fig. 8. FTIR spectra of Cys, AgGSH, AgGSHCys, and AgGSHNi^{2+}Cys.

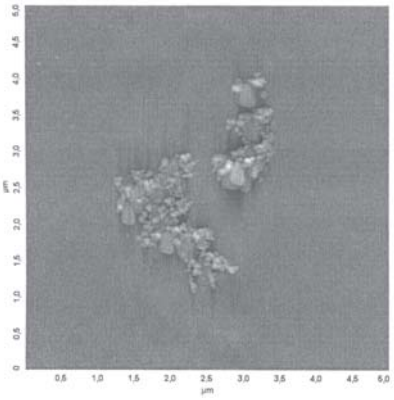

Fig. 9. AFM topographical image of the AgGSHNi^{2+}Cys complex. mediated by 0.001 M GSH, deposited on a glass after dispersing in methanol and scanner area is 25 μm^2

detection limit of the complex, a series of Cys solutions with different concentrations ranging from 1×10^{-5} to 1×10^{-3} M were added to the mixture solution (fig. 7). A linear relationship exists between the absorbance of the solution at 270.1 nm and the Cys concentration in the range between 1×10^{-4} and 1×10^{-3} M with the detection limit of 1×10^{-5} M. Li et al. [27] have reported that the interaction between cysteine and gold nanoparticles which result in resonance light scattering. They demonstrated that the linear range of determination of cysteine is from 0.01 to 0.25 μg/mL. It was reported that near infrared fluorescent dye FR 730 adsorbed gold nanoparticles and cysteine interaction which result in quenching fluorescence intensity [28]. The reported linear range for determination of cysteine is $2.5x10^{-8}$ – $4x10^{-6}$ M. Was demonstrated that carboxymethyl cellulose modified gold nanoparticles and cysteine interaction which result in particle aggregation at the presence of sodium chloride [38]. The obtained linear range for determination of cysteine is 10 – 100 μM with the basis of UV-vis absorption measurements. The range of cysteine concentration obtained in this study considered satisfactory compared the results reported by mentioned other literature works. The all of the mentioned literature works and this study have good selectivity and sensitivity because of the strong affinity of thiols to gold and silver nanoparticles.

Characterization of AgGSHNi^{2+}Cys structure

Evidence for the presence of surface-bound Cys is provided by FTIR measurements of Cys, AgGSH, AgGSH-Cys, and AgGSH-Ni^{2+}-Cys in the range of 600–4000 cm^{-1}. To investigate the mechanisms of the interaction, 1×10^{-3} M Cys solution was added to the AgGSH solution and the resulting structure was analyzed by FTIR (fig. 8). The free Cys residue shows a characteristic band at ~2540 cm^{-1} owing to the presence of the -SH group.

The complete disappearance of the -SH stretching band at 2540 cm^{-1} indicates covalent interaction between Cys and the AgGSH nanoparticles through the sulfydryl bond [39]. In the AgGSH-Ni^{2+}Cys FTIR spectrum, the carboxylate asymmetric and symmetric stretching vibrational bands overlap with the stronger nitrate vibrational bands in $Ni(NO_3)_2$ at 1284 cm^{-1} and 1339 cm^{-1}. In the AgGSH-Ni^{2+}-Cys FTIR spectra, the NH_3^+ and -COO$^-$ vibrational absorption bands on the glutamate moiety at 3343 and 1570 cm^{-1}, respectively, appear at 3343 and 1573 cm^{-1}, respectively, suggesting that these groups do not participate in the complex formation. On the other hand, the amide groups of the AgGSH complex and the carboxylate and amine groups of Cys form a complex with the Ni^{2+} ions, inducing a new absorption band at 270 nm. In the 2D-topographic AFM image of the AgGSH-Ni^{2+}Cys complex, shown in figure 9 particle aggregation is observed because the glutamate zwitterion interacts with the other particles via -COO$^-$ and -NH^{3+}. As seen in Fig. 9 some nanoparticle heaps are composed due to lots of interacting groups.

Conclusions

We have demonstrated a new Cys detection method based on glutathione-capped silver nanoparticles. Adsorption of GSH to the silver nanoparticles occurred via the -SH group of cysteine and the -COO$^-$ group of glycine. An AgGSH-Ni^{2+}-Cys complex is formed by interactions with amide groups of AgGSH, Ni^{2+} ions, and amide and carboxilate groups of Cys. The complex shows a new absorption band at 270.1 nm and this band enables selective detection of cysteine. A linear relationship exists between the absorption at 270.1 nm and the concentration of Cys in the range 1×10^{-4} and 1×10^{-3} M. Furthermore, the Cys detection limit is 1×10^{-5} M.

Acknowledgments: This work was financially supported by the Sakarya University Commission of Scientific Research Projects (Project number: 2010.50.02.006).

References

1. ROSSI, L M, QUACH, A D, ROSENZWEIG, Z., Anal. Bioanal Chem., **380**, 2004, p.606.
2. HAN, J., SILCOCK, P., MCQUILLAN, A. J., BREMER, P., Colloids and Surfaces A: Physicochem. Eng. Aspects, **349**, 2009, 207.
3. HE. F., ZHAO. D., PAUL. C., Water Research, **44**, 2010, p.2360.
4. KOMMAREDDY, S., AMIJI, M, Bioconjugate Chem. **16**, 2005, p.1423.

5. DEMERS, L. M., MIRKIN, C. A., MUCIC, R. C., REYNOLDS, R. A., LETSINGER, R. L., ELGHANIAN, R., VISWANADHAM, G., Anal. Chem., **72**, 2000, p.5535.
6. CHOMPOOSOR, A., HAN, G., AND ROTELLO, V. M., Bioconjugate Chem., **19**, 2008, p.1342.
7. VARGHESE, M. V., DHUMAL, R. S., PATIL, S. S., PARADKAR, A. R. AND KHANNA, P. K., Synthesis and Reactivity in Inorganic, Metal-Organic, and Nano-Metal Chemistry, **39**, 2009, p.554.
8. BRELLE, M. C., ZHANG, J. Z., NGUYEN, L., AND MEHRA. R, K, J. Phys. Chem. A, **103,** 1999, p.10194.
9. KREZEL, A., AND BAL, W., Bioinorganic Chemistry and Applications, **2**, 2004, p.3.
10. NGUYEN, L., KHO, R., BAE, W. AND MEHRA, R. K., Chemosphere, **38**, 1999, p.155.
11. ZHENG, Y., GAO, S., YING, J. Y., Adv. Mater. **19**, 2007, p.376.
12. LI, H., CUI, Z., HAN, C., Sensors and Actuators B, **143**, 2009, p.87.
13. SANTHIAGO, M., LIMA, P.R., SANTOS, W.J.R., KUBOTA, L.T., Sensors and Actuators B, 146, 2010, p.213.
14. SANTHIAGO, M., VIEIRA, I.C., Sensors and Actuators B, **128**, 2007, p.279.
15. LAU, C., QIN, X., LIANG, J., LU, J., Analytica Chimica Acta, **514**, 2004, p.45.
16. CHWATKO, G. AND BALD, E., Talanta, **52**, 2000, p.509.
17. NAMERA, A., YASHIKI, M., NISHIDA, M., AND KOJIMA, T., Journal of Chromatography B, **776,** 2002, p.49.
18. ANDERSSON, A., BRATTSTROM, L., ISAKSSON, A., ISRAELSSON, B., ULTBERG, B., Scand J Clin Lab Invest, **49**, 1989, p.445.
19. GAITONDE, M. K., Biochem. J., **104**, 1967, p.627.
20. BERTAGNOLLI, B. L. AND WEDDING, R. T., J. Nutr., **107**, 1977, p.2122.
21. AVI-DOR, Y., MAGER, J., The Journal of Biological Chemistry, **222**, 1956, p.249.
22. HESS, W. C. SULLIVAN, M**.** X., The Journal of Biological Chemistry, **108**, 1934, p.195.
23. NIE, L., MA, H., SUN, M., LI, X., SU, M., LIANG, S., Talanta, **59**, 2003, p.959.
24. DROZDZ, R., NASKALSKI, J. AND Z BEK-ADAMSKA, A., Acta Biochimica Polonica, **54**, 2007, p.205.
25. SPATARU, N., SARADA, B. V., POPA, E., TRYK, D. A., AND FUJISHIMA, A., Anal. Chem., **73**, 2001, p.514.
26. KANG, S. H., WEI, W., AND YEUNG, E. S., Journal of Chromatography B, **744**, 2000, p.149.
27. LI, Z. P., DUAN, X. R., LIU, H. C., DU, B. A., Analytical Biochemistry, **351**, 2006, p.18.
28. SHANG, LI, YIN J, LI J, JIN L, DONG S., Biosensors and Bioelectronics, **25,** 2009, 269-274.
29. SUDEEP, P.K., JOSEPH, S.T.S., AND THOMAS, K.G., J. Am. Chem. Soc., **127**, 2005, p.6516.
30. LI, H. AND BIAN, Y., Nanotechnology, **20**, 2009, p.1
31. MANDAL, S., GOLE, A., LALA, N., GONNADE, R., GANVIR, V., AND SASTRY, M., Langmuir, **17**, 2001, p.6262.
32. BIERI, M. AND BÜRGI, T., Langmuir, **21**, 2005, p.1354.
33. BASU, S., GHOSH, S.K., KUNDU, S., PANIGRAHI, S., PRAHARAJ, S., PANDE, S., JANA, S., AND PAL, T., Journal of Colloid and Interface Science, **313**, 2007, p.724.
34. LIM, I.S., MOTT, D., IP, W., NJOKI, P.N., PAN, Y., ZHOU, S., AND ZHONG, C. J., Langmuir, **24**, 2008, p.8857.
35. SILVER, J., HAMED, M.Y. AND MORRISON, I.E.G., Inorg Chim Acta, **107**, 1985, p.169.
36. SHINDO, H. AND BROWN, T.L., J Am Chem. Soc, **87**, 1965, p.1904.
37. PETEAN, I., TOMOAIA, G.H., HOROVITZ, O., MOCANU, A., AND TOMOAIA-COTISEL, M., Journal of Optoelectronics and Advanced Materials, **10**, 2008, p.2289.
38. WEI, X., QI, L., TAN, J., LIU, R., WANG, F., Analytica Chimica Acta, **671**, 2010, p80.
39. CHOI, S., LEE, S., HWANG, Y., LEEA, K., KANG, H., Radiation Physics and Chemistry, **67**, 2003, p.517

Manuscript received: 17.07.2011